Title
Chemoproteomics-enabled discovery of a covalent molecular glue degrader targeting NF-κB

Journal
Cell Chemical Biology, 30(4)

ISSN
2451-9456

Authors
King, Elizabeth A
Cho, Yoojin
Hsu, Nathan S
et al.

Publication Date
2023-04-01

DOI
10.1016/j.chembiol.2023.02.008

Peer reviewed

HHS Public Access

Author manuscript

Cell Chem Biol. Author manuscript; available in PMC 2024 April 20.

Chemoproteomics-Enabled Discovery of a Covalent Molecular Glue Degrader Targeting NF-κB

Elizabeth A. King[1,2,3], **Yoojin Cho**[1,2,3], **Nathan S. Hsu**[1,2,3], **Dustin Dovala**[2,4], **Jeffrey M. McKenna**[2,5], **John A. Tallarico**[2,5], **Markus Schirle**[2,5], **Daniel K. Nomura**[1,2,3,6,*]

[1]Department of Chemistry, University of California, Berkeley, Berkeley, CA 94720 USA

[2]Novartis-Berkeley Center for Proteomics and Chemistry Technologies

[3]Innovative Genomics Institute, Berkeley, CA 94704 USA

[4]Novartis Institutes for BioMedical Research, Emeryville, CA 94608 USA

[5]Novartis Institutes for BioMedical Research, Cambridge, MA 02139 USA

[6]Department of Molecular and Cell Biology, University of California, Berkeley, Berkeley, CA 94720 USA

Summary

Targeted protein degradation has arisen as a powerful therapeutic modality for degrading disease targets. While Proteolysis Targeting Chimera (PROTAC) design is more modular, the discovery of molecular glue degraders has been more challenging. Here, we have coupled the phenotypic screening of a covalent ligand library with chemoproteomic approaches to rapidly discover a covalent molecular glue degrader and associated mechanisms. We have identified a cysteine-reactive covalent ligand EN450 that impairs leukemia cell viability in a NEDDylation and proteasome-dependent manner. Chemoproteomic profiling revealed covalent interaction of EN450 with an allosteric C111 in the E2 ubiquitin conjugating enzyme UBE2D. Quantitative proteomic profiling revealed the degradation of the oncogenic transcription factor NFKB1 as a putative degradation target. Our study thus puts forth the discovery of a covalent molecular glue degrader that uniquely induced the proximity of an E2 with a transcription factor to induce its degradation in cancer cells.

Graphical Abstract

*Lead Contact: dnomura@berkeley.edu.

Author Contributions

EAK, DKN conceived of the project idea, designed experiments, performed experiments, analyzed and interpreted the data, and wrote the paper. EAK, YC, NSH, DD, DKN performed experiments, analyzed and interpreted data, and provided intellectual contributions. EAK, DD, JAT, JMK, MS provided intellectual contributions to the project and overall design of the project.

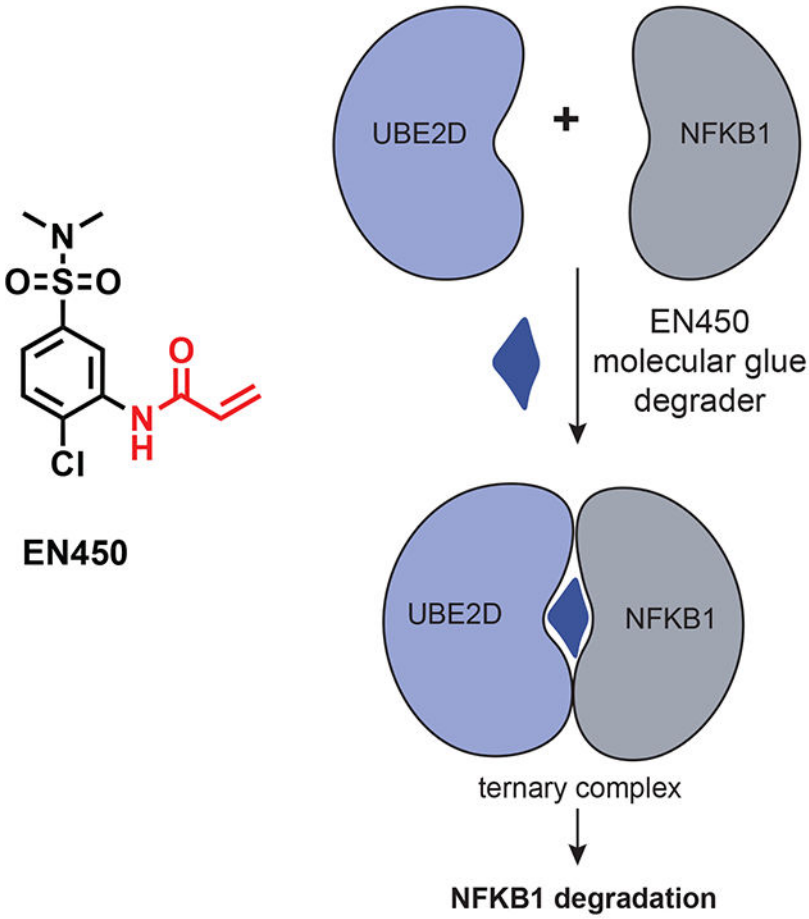

eTOC Blurb

King et al. used phenotypic screening and chemoproteomic approaches to discover a covalent molecular glue degrader, EN450. EN450 is a cysteine reactive covalent ligand that uniquely induced the proximity of an E2 ubiquitin conjugating enzyme UBE2D with the oncogenic transcription factor NFKB1 to induce its degradation in cancer cells.

Keywords

activity-based protein profiling; targeted protein degradation; molecular glue; E2 ligase; UBE2D; NFKB1; transcription factor

Introduction

Most small-molecule drugs in the clinic operate through classical occupancy-driven pharmacology that consists of small-molecules binding to deep active site binding pockets and resulting in functional modulation of the target. However, many therapeutic target proteins have been deemed “undruggable” since they do not possess well-defined, functionally relevant binding pockets, thus rendering these proteins inaccessible to classical drug discovery approaches [1,2]. Targeted protein degradation using heterobifunctional

Proteolysis-Targeting Chimeras (PROTACs) or molecular glues has arisen as a powerful alternative therapeutic modality aiming at degradation instead of inhibition of the disease target [3,4]. While heterobifunctional PROTACs still require protein-targeting ligands that are capable of binding to the target protein with decent potency, monovalent molecular glue degraders can exploit shallower protein interfaces to induce ternary complex formation and subsequent ubiquitination and degradation of specific proteins [5]. While molecular glue degraders are potentially more attractive and drug-like, most molecular glue degraders have been discovered fortuitously and rational discovery of molecular glue degraders has remained challenging.

Recent studies by Mayor-Ruiz and Winter *et al.* have showcased innovative phenotypic screening paradigms for rapidly discovering small-molecules that exert anti-cancer activity through molecular glue degrader mechanisms [6]. These screens for anti-cancer small-molecules consisted of counter screens for an attenuated phenotype in hyponeddylation cell lines to identify molecules that exerted their phenotypes through a Cullin E3 ligase-dependent mechanism. However, the backend mechanistic elucidation of the ternary complex components—identifying the degraded target and ubiquitin-proteasome component that were brought together by the small-molecule—required whole genome-wide CRISPR screens which can sometimes be laborious and may yield indirect targets in addition to direct targets of the small-molecule [6].

Covalent chemoproteomic approaches have arisen as powerful platforms for coupling phenotypic screening of covalent electrophile libraries with rapid mechanistic deconvolution [1,7–11]. As such, we conjectured that coupling the screening of a covalent ligand library for molecular glue degraders with backend chemoproteomic and quantitative proteomic approaches would provide rapid discovery of molecular glue degraders and their ternary complex components and downstream mechanisms. In this study, we phenotypically screened a library of covalent ligands for antiproliferative compounds and used chemoproteomic platforms to discover a covalent molecular glue degrader that uniquely relies on an E2 ubiquitin conjugating enzyme.

Results

To discover covalent molecular glue degraders, we screened a library of 750 cysteine-reactive covalent ligands for anti-proliferative effects in HAP1 leukemia cancer cells (Figure 1a; Table S1). We identified 11 hits from our primary screen, of which 3 of these hits—EN222, EN450, and EN266—showed reproducible impairments in HAP1 cell proliferation by greater than 90% (Figure 1b). Among these three hits, we next sought to identify if these compounds may be exerting their anti-proliferative effects through a Cullin E3 ubiquitin ligase-dependent mechanism. To this end, we counter-screened our hit compounds in UBE2M knockdown hyponeddylation lines alongside dCeMM1, a positive control molecular glue degrader previously identified by Mayor-Ruiz and Winter *et al.* which induces degradation of RBM39 in a $CRL4^{DCAF15}$-dependent manner (Figure 1c–1d) [6]. NEDDylation is a critical post-translational modification necessary for the activity of all Cullin E3 ligases [12]. As such, compounds that show attenuated phenotypes in these hyponeddylation cell lines would indicate a Cullin E3 ligase-dependent mechanism.

EN266, EN450, and the positive control glue degrader dCeMM1, but not EN222, showed significant attenuation of anti-proliferative effects in HAP1 cells with EN450 showing the most robust effects (Figure 1d–1e). EN450 is a fragment ligand containing a cysteine-reactive acrylamide warhead (Figure 1e). EN450 as well as dCeMM1 also showed significant attenuation of anti-proliferative effects upon pre-treatment of HAP1 cells with the NEDDylation inhibitor MLN4924 and the proteasome inhibitor bortezomib, further cementing that EN450 was exerting its anti-proliferative effects through a Cullin E3 ligase and proteasome-dependent mechanism (Figure 1f–1g).

Based on these data, we conjectured that EN450 was a molecular glue inducing the proximity of a target protein with a component of the ubiquitin-proteasome system (UPS) to form a ternary complex leading to the ubiquitination and proteasome-mediated degradation of the target protein and subsequent anti-proliferative effects in HAP1 cells. To identify proteome-wide covalent targets of EN450, we performed cysteine chemoproteomic profiling using isotopic tandem orthogonal proteolysis-activity-based protein profiling (isoTOP-ABPP) [7,13]. Through competitive profiling of EN450 covalent protein targeting in HAP1 cells against cysteine-reactive alkyne-functionalized iodoacetamide probe labeling, we identified 81 targets that showed significant engagement—control/EN450-treated ratio of >1.3 with adjusted p-values <0.05—among 4501 cysteines quantified (Figure 2a; Table S2). Given that we and others have previously shown that the UPS is highly ligandable with covalent ligands, that even partial covalent occupancy of a UPS effector protein can lead to significant degradation of the target protein due to the catalytic nature of degraders, and that EN450 is a small-molecule fragment that is not likely to engage in high-affinity interactions, we conjectured that the covalent interaction of EN450 is likely occurring with a component of the ubiquitin-proteasome system, rather than the target protein [10,14–18]. Because of these reasons, we purposefully chose a low ratio cut-off since we did not want to miss low-occupancy targets of EN450 [10,16,19]. Among these targets, only one protein was involved in the UPS and the Cullin E3 ligase machinery—C111 of ubiquitin-conjugating enzyme E2D (UBE2D). C111 is an allosteric cysteine in UBE2D that is distal from the cysteine (C85) that undergoes ubiquitin conjugation during ubiquitin transfer. Because of the high degree of sequence identity between UBE2D isoforms, we could not distinguish whether EN450 targeted C111 on UBE2D1, UBE2D2, UBE2D3, or UBE2D4. Nonetheless, UBE2D is one of the key E2 ligases that are coupled with the Cullin E3 ligase complex, which is consistent with attenuation of EN450 anti-proliferative effects with a NEDDylation inhibitor of Cullin E3 ligases [12].

To further characterize interactions of EN450 with UBE2D, we synthesized an alkyne-functionalized probe derivative of EN450—EK-1-8 (Figure 2b). EK-1-8 still impaired HAP1 cell viability in a NEDDylation-dependent manner (Figure 2c). EK-1-8 directly and covalently labeled recombinant UBE2D1 C85S mutant protein in a dose-responsive manner (Figure 2d). This labeling was attenuated, albeit not completely, upon mutation of both C85 and C111 on UBE2D1 to serines (Figure S1a). We interpreted the residual labeling evident in the double mutant as another allosteric cysteine on UBE2D1 that may be additionally reactive with EN450, potentially in the absence of its main reactive C111. We further demonstrated that EK-1-8 engaged UBE2D1, but not an unrelated protein such as GAPDH, in HAP1 cells and that this engagement was outcompeted in-part by EN450,

as assessed by enrichment of UBE2D1 in HAP1 cells by EK-1-8 treatment, appendage of biotin through azide-alkyne cycloaddition (CuAAC), avidin-enrichment, elution, and blotting (Figure 2e). We also synthesized the non-reactive analog of EN450, EK-1-37, as well as its alkyne-functionalized derivative, EK-1-38, to ascertain the contribution of the covalent acrylamide warhead to the observed effects (Figure. S1b). EK-1-37 did not impair HAP1 cell viability and EK-1-38 expectedly did not show any covalent modification of UBE2D1 C85S, compared to EK-1-8 (Figure S1c–S1d).

To understand the contribution of the individual UBE2D isoforms to EN450 effects, we assessed dose-responsive effects of EN450 on HAP1 cell proliferation upon knockdown of UBE2D1, UBE2D2, UBE2D3, and UBE2D4 and knockdown of all four enzymes (Figure 2f–2g, Figure S2). Knockdown of UBE2D1 conferred the greatest degree of resistance to EN450 antiproliferative effects, followed by knockdown of UBE2D4 and knockdown of all four enzymes. Intriguingly, knockdown of UBE2D2 and UBE2D3 led to hypersensitization to EN450, suggesting divergent roles of each individual E2 ligase isoform in relation to interactions with EN450 despite their high degree of sequence identity (Figure 2f–2g, Figure S1). Nonetheless, our data indicated that UBE2D1 and UBE2D4 are likely the UPS components covalently engaged by EN450 to, presumably along with the recruitment of its associated Cullin E3 ligase complex, ubiquitinate and degrade a yet unknown target protein to exert its antiproliferative effects.

To identify the degraded target protein, we next performed tandem mass tagging (TMT)-based quantitative proteomic profiling to map protein level changes from EN450 treatment in HAP1 cells. This profiling effort revealed only one protein—the NFKB1 p105 subunit—that was significantly reduced in levels by >4-fold upon EN450 treatment compared to vehicle-treated controls (Figure 3a; Table S3). Loss of both the precursor p105 protein and further processed p50 product of NFKB1 was confirmed by Western blotting (Figure 3b–3d). The non-reactive EK-1-37 control did not lower NFKB1 levels (Figure S3a). We further confirmed that the reduction in NFKB1 p105 and p50 levels by EN450 treatment was not observed when HAP1 cells were pre-treated with the NEDDylation inhibitor (Figure 3e–3f). MLN4924 treatment itself, reduced NFKB1 levels potentially due to its inherent toxicity in leukemia cancer cells [20], but EN450 did not further lower NFKB1 levels (Figure 3e–3f).

Next, we sought to demonstrate EN450-mediated ternary complex formation between UBE2D and NFKB1. First, we demonstrated that EN450 promoted ternary complex formation between UBE2D1 and NFKB1, through pulldown studies with recombinant GST-NFKB1 and UBE2D1 protein (Figure 3g–3h). We then showed that both p105 and p50 NFKB1 isoforms, but not an unrelated GAPDH control, were pulled down by EK-1-8 from HAP1 cells in addition to our previously described results showing pulldown of UBE2D1 (Figure 2e, Figure S3b). Third, reconstitution of UBE2D1-mediated ubiquitination activity showed that EN450 enhanced ubiquitination of NFKB1 only in the presence of the full CUL4A/RBX1/NEDD8 complex (Figure 3i–3j). We also demonstrated that UBE2D1 knockdown alone has no influence on NFKB1 levels (Figure S3c). Overall, these results were consistent with EN450 forming a productive ternary complex between UBE2D and NFKB1 in cells that resulted in NFKB1 ubiquitination and degradation.

EN450 is clearly not a selective compound as demonstrated by ~80 potential cysteine targets identified by chemoproteomic profiling. Nonetheless, we sought to link the degradation of NFKB1, a known oncogenic transcription factor [21], to the mechanism underlying EN450 anti-proliferative effects. Stable overexpression of NFKB1 in HAP1 cells led to significant attenuation of EN450-mediated anti-proliferative effects in a dose-dependent manner (Figure 4a–4b). We also transiently transfected NFKB1 in HEK293T cells, where we also demonstrated NEDDylation-dependent cell viability impairments and reduction in NFKB1 levels with EN450 treatment (Figure 4d–4e). We observed an even more robust rescue of EN450-mediated anti-proliferative effects (Figure 4f). While we believe that EN450 likely has additional polypharmacological mechanisms underlying its anti-proliferative effects, our data suggest that NFKB1 is at least partially involved in the anticancer effects of EN450.

Discussion

In this study, we have used covalent chemoproteomic approaches to discover a covalent molecular glue degrader that uniquely induces the proximity of an E2 conjugating enzyme UBE2D1 to the oncogenic nuclear transcription factor NFKB1 to ubiquitinate and degrade NFKB1 in a proteasome and NEDDylation-dependent manner. Our study also reveals that allosteric sites within E2 ubiquitin conjugating enzymes, rather than E3 ligases or E3 ligase substrate receptor or adapter proteins, can be directly targeted by small-molecules to engage in molecular glue interactions with neo-substrate proteins. Our study is reminiscent of previously reported studies by Slabicki and Ebert *et al.* demonstrating that the CDK8 inhibitor CR8 acts as a molecular glue degrader of cyclin K through engaging a core adapter protein of the CUL4 E3 ligase machinery DDB1, thereby bypassing the requirement for a substrate receptor for ubiquitination and degradation [23]. Both our and the Ebert study demonstrate that core proteins within the ubiquitin proteasome machinery, such as E2 ligases and DDB1, can be exploited for targeted protein degradation application. This indicates that small-molecule recruiters can be developed against these core components of the UPS for use in heterobifunctional degraders. While this paper was under revision, we also demonstrated that both EN450 and more potent UBE2D covalent recruiters could be used in PROTACs to degrade neo-substrate proteins [24]. Taken more broadly, our study also demonstrates the utility of coupling covalent ligand screening with chemoproteomic and quantitative proteomic platforms to rapidly discover molecular glue degraders and their ternary complex components. Furthermore, we may identify even more molecular glue degraders through the development of bespoke compound collections, including covalent enantiopair libraries [11,25] or covalent macrocycles [26], and by coupling these specialized libraries with not only chemoproteomic platforms but also target-based cellular screens or size-exclusion chromatography [25].

Limitations of the Study

Our study reveals a covalent molecular glue degrader that engages the E2 ubiquitin conjugating enzyme UBE2D to engage in molecular glue interactions with NFKB1 leading to the degradation of NFKB1 in cancer cells. Our study nonetheless still has several limitations and open questions. While the NEDDylation-dependency indicates that UBE2D still needs to be coupled to the Cullin E3 ligase complex to mark NFKB1

for degradation and confer anti-proliferative effects based on the attenuation of these effects by a NEDDylation inhibitor, we do not yet know whether recruitment of the E2 bypasses the necessity for a substrate adapter protein to induce the ubiquitination and degradation of NFKB1. We also acknowledge that the NEDDylated CUL4/RBX1 used to reconstitute the ternary complex here is not the ideal RING E3 ligase to address the role of C111 on UBE2D1 on the activated structure since NEDD8 binds UBE2D. As such, the ubiquitination activity that we observe may not exclusively rely on the RING causing the folded back UBE2D1-ubiquitin arrangement, as described in previous literature [22]. We also note that due to limitations on garnering sufficient pure protein to perform all necessary control experiments for the reconstitution assays, we were not able to test negative control compounds in these assays, and as such cannot exclude an effect of the small-molecule beyond what we hypothesized. The mechanism for NFKB1 degradation may also operate through initial mono-ubiquitination of NFKB1 through the EN450-mediated UBE2D/NFKB1 molecular glue interaction that subsequently sensitizes NFKB1 to polyubiquitination and degradation through a combination of or specific E3 ligases. Of future interest is the investigation of whether NFKB1 already interacts weakly with this allosteric site on UBE2D, and whether EN450 thus just strengthens an already existing interaction or whether NFKB1 truly represents a neo-substrate that engages UBE2D only upon EN450 binding. While we demonstrate here that EN450 directly engages with UBE2D1 alone without NFKB1, it is unclear at this point whether EN450 has any inherent reversible affinity for NFKB1 or whether UBE2D1 binding to EN450 is necessary to recruit NFKB1. We acknowledge that EN450 is a primary screening hit that is not selective or potent enough and likely has polypharmacological action in cancer cells. Future improved UBE2D-based NFKB1 degraders can potentially be used to identify particularly sensitive cancer cells that may respond therapeutically to NFKB1 degradation beyond leukemias.

STAR METHODS

Resource Availability

Lead Contact: Further information and requests for resources and reagents should be directed to and will be fulfilled by the lead contact, Daniel K. Nomura (dnomura@berkeley.edu).

Materials availability: Compounds and protocols generated in this study will be available upon request. Any raw data or images generated in this proposal will be provided upon request.

Data and code availability:

- All proteomic raw data files are available via ProteomeXchange with Project accession PXD039924. The mass spectrometry proteomics data have been deposited to the ProteomeXchange Consortium via the PRIDE partner repository with the database identifier PXD039924.
- Data processing and statistical analysis algorithms for chemoproteomics from our lab can be found on our lab's Github site: https://github.com/NomuraRG, and we can make any further code from this study available upon request.

- Any additional information required to reanalyze the data reported in this paper is available from the lead contact upon request.

Experimental Model and Subject Details

Cell Culture—HAP1 cells were purchased from Horizon Discovery and were cultured in IMDM containing 10% (v/v) fetal bovine serum (FBS) and maintained at 37 °C with 5% CO_2. HAP1 cells are male in origin. HEK293T cells were obtained from the American Type Culture Continued. HEK293 cells were originally derived from a female fetus but the sex is unclear. HEK293T cells were cultured in DMEM containing 10% (v/v) fetal bovine serum (FBS) and maintained at 37° C with 5% CO_2. Unless otherwise specified, all cell culture materials were purchased from Gibco. It is not known whether HEK293T cells are from male or female origin.

Method Details

Materials—Cysteine-reactive covalent ligand libraries were either previously synthesized and described or for the compounds starting with “EN” were purchased from Enamine, including EN450. Other chemicals synthesized for this study are described in Supporting Information.

Preparation of Cell Lysates—Cells were washed twice with cold PBS, scraped, and pelleted by centrifugation (1,400 *g*, 4 min, 4° C). Pellets were resuspended in PBS containing protease inhibitor cocktail (ThermoFisher A32955), sonicated, clarified by centrifugation (21,000 *g*, 10 min, 4° C), and lysate was transferred to another low-adhesion microcentrifuge tubes. Proteome concentrations were determined using BCA assay and lysate was diluted to appropriate working concentrations.

Cell Viability—Cell viability assays were performed using Hoechst 33342 dye (Invitrogen H3570) according to the manufacturer’s protocol. For survival assays, cells were seeded into 96-well plates (20,000 per well) in a volume of 100 μL and allowed to adhere overnight, cells were treated with an additional 50 μL of media containing DMSO vehicle or compound (150 μM) in 0.1% DMSO for 24 h. For rescue experiments, cell media was changed to media (100 μL per well) containing Bortezomib (1 μM) (Calbiochem 5043140001) or MLN4924 (1 μM) (Calbiochem 5054770001) for 1 h prior to compound treatment. For dose response experiments, dilutions of compound were prepared in DMSO prior to dilution in media. After incubation, the media was aspirated from each well, and 100 μL of staining solution containing 10% formalin and Hoechst 33342 dye (Invitrogen H3570) was added to each well and incubated for 25 min in the dark at room temperature. Staining solution was then removed, and wells were washed with 3x with PBS before fluorescent imaging.

Production of Recombinant UBE2D1—A UBE2D1(1-147) expression plasmid was synthesized by Twist Biosciences with an N-terminal 8xHistidine tag and HRV 3C cleavage site. The C85S and C111S mutations were produced using a Q5 Site Directed Mutagenesis Kit (New England Biolabs E0554S) and standard cloning techniques. HI-Control BL21(DE3) *E. coli* cells (Lucigen 60435-1) were transformed with expression plasmid and a single colony was used to start an overnight culture in LB media, followed by

inoculation of a 1 L culture in Terrific Broth supplemented with 50 mM sodium phosphate monobasic pH 7.0 and 50 μg/mL kanamycin. This culture grew at 37 °C until the OD600 reached approximately 1.2, at which point the temperature was reduced to 19 °C along with immediate addition of 0.5 mM (final) IPTG. The cells were allowed to grow overnight prior to harvesting via centrifugation. The cell pellet was resuspended in IMAC_A Buffer (50 mM Tris pH 8.0, 400 mM NaCl, 1 mM TCEP, 20 mM imidazole) and lysed with three passages through a cell homogenizer at 18,000 psi. Cell lysate was then clarified with centrifugation at 45,000 x g for 30 minutes. The clarified lysate was flowed through a 5 mL HisTrap Excel column (Cytiva) pre-equilibrated with IMAC_A Buffer. After loading, the resin was washed with IMAC_A Buffer until the UV absorbance reached baseline, after which the protein was eluted with a linear gradient of IMAC_B Buffer (50 mM Tris pH 8.0, 400 mM NaCl, 1 mM TCEP, 500 mM imidazole). The eluate was treated with HRV 3C protease until cleavage of the histidine tag was complete as determined by ESI-LC/MS. Cleavage proceeded while the protein dialyzed into IMAC_A Buffer, enabling reverse-IMAC purification which was conducted in batch using 3 mL of Ni-NTA resin pre-equilibrated with IMAC_A Buffer. The flow-through was collected, concentrated, and subjected to size exclusion chromatography using a Superdex 75 16/600 column (Cytiva) pre-equilibrated with SEC Buffer (25 mM HEPES pH 7.5, 150 mM NaCl, 1 mM TCEP). Fractions within the included volume were analyzed by SDS-PAGE and those containing pure protein were pooled and concentrated. This protocol was used to produce wild-type, C85S, and C85S/C111S variants of UBE2D1 with an approximate yield of ~90 mg/L.

Labeling of Recombinant UBE2D1 with EK-1-8 and EK-1-38 Probes—For in vitro labelling of UBE2D1 C85S, recombinant pure human protein (0.1 μg per sample) was treated with either DMSO vehicle, EK-1-8, or EK-1-38 at 37° C for 30 min in 25 μL PBS. Each sample was incubated with 1 μL of 30 μM rhodamine-azide (in DMSO) (Click Chemistry Tools AZ109-5), 1 μL of 50 mM TCEP (in water) (Strem 15-7400), 3 μL of TBTA ligand (0.9 mg/mL in 1:4 DMSO/*t*-BuOH) (Sigma 678937), and 1 μL of 50 mM Copper (II) Sulfate (Sigma 451657) for 1 h at room temperature. Samples were then diluted with 10 μL of 4x reducing Laemmli SDS sample loading buffer (Alfa Aesar J60015), boiled at 95° C for 5 min, and separated by SDS/PAGE. Probe-labeled proteins were analyzed by in-gel rhodamine fluorescence using a ChemiDoc MP (Bio-Rad). Protein loading was assessed by silver staining.

Pulldown of UBE2D1 from HAP1 Cells with EK-1-8 Probe—HAP1 WT cells were pretreated at 70% confluency with DMSO or 50 μM EN450 in situ for 1 h followed by treatment with DMSO or 10 μM EK-1-8 in situ for 3 h . Cells were harvested, lysed via sonication, and the resulting lysate normalized to 6 mg/mL per sample. Following normalization, 30 μL of each lysate sample was removed for Western blot analysis of input, and 500 μL of each lysate sample was incubated for 2 h at room temperature with 10 μL of 5 mM biotin picolyl azide (in DMSO) (Sigma Aldrich 900912), 10 μL of 50 mM TCEP (in water), 30 μL of TBTA ligand (0.9mg/mL in 1:4 DMSO/*t*-BuOH), and 10 μL of 50 mM Copper (II) Sulfate. Proteins were precipitated, washed 3 x with cold MeOH, resolubilized in 200 μL of 1.2% SDS/PBS (w/v), heated for 5 min at 98 C, and centrifuged to remove any insoluble components. Each resolubilized sample was then transferred to

1.5 mL eppendorf low-adhesion tubes containing 1 mL PBS with 30 μL high-capacity streptavidin resin (ThermoFisher 20357) to give a final SDS concentration of 0.2%. Samples were incubated with the streptavidin beads at 4° C overnight on a rotator. The following day the samples were warmed to room temperature and washed with 0.2% SDS and further washed 3 x with 500 μL PBS and 3 x with 500 μL water to remove non-probe-labeled proteins. For western blot analysis, the washed beads were resuspended in 30 μL PBS, transferred to 1.5 mL eppendorf low-adhesion tubes, combined with 10 μL Laemmli Sample Buffer (4 x), heated to 95° C for 5 min, and analyzed by Western blotting to look for enriched UBE2D1 versus non-enriched control Vinculin.

Western Blotting—Antibodies to NFKB p105/p52 (Abcam ab323670), SFT (Abcam ab176561), UBE2D2 (Origene TA806600), UBE2D3 (Abcam ab176568), UBE2D4 (Invitrogen MA5-27358), UBE2M/UBC12 (Abcam ab109507), DYKDDDDK Tag (D6W5B) (Cell Signaling Technology Cat#14793S), Vinculin (Bio-Rad Cat#MCA465S), GAPDH (Proteintech Cat#60004-I-Ig) were obtained commercially and prepared at dilutions recommended by the manufacturers. Proteins were resolved by SDS/PAGE and transferred to nitrocellulose membranes using the Trans-Blot Turbo transfer system (Bio-Rad). Membranes were blocked with 5% BSA in Tris-buffered saline containing Tween 20 (TBS-T) solution for 30 min at RT, washed in TBS-T, and probed with primary antibody diluted 5% BSA in TBS-T overnight at 4°C. After 3 washes with TBS-T, the membranes were incubated in the dark with IR680- or IR800-conjugated secondary antibodies obtained commercially from LI-COR at 1:10,000 dilution in 5 % BSA in TBS-T at RT for 1 h. After 3 additional washes with TBST, blots were visualized using an Odyssey Li-Cor fluorescent scanner. The membranes were stripped using ReBlot Plus Strong Antibody Stripping Solution (EMD Millipore) when additional primary antibody incubations were performed.

IsoTOP-ABPP Chemoproteomic Profiling—IsoTOP-ABPP studies were done as previously reported [13,26,27]. Cells were treated for 3 h with either DMSO vehicle or EN450 (50 uM) before cell lysate preparation as described above. Proteomes were subsequently labeled with IA-alkyne labeling (200 μM) (Chess Gmbh 3187) for 1 h at room temperature. CuAAC was used by sequential addition of tris(2-carboxyethyl)phosphine (1 mM), tris[(1-benzyl-1H-1,2,3-triazol-4-yl)methyl]amine (34 μM), copper(II) sulfate (1 mM) and biotin-linker-azide—the linker functionalized with a tobacco etch virus (TEV) protease recognition sequence as well as an isotopically light or heavy valine for treatment of control or treated proteome, respectively. After CuAAC, proteomes were precipitated by centrifugation at 6,500g, washed in ice-cold methanol, combined in a 1:1 control treated ratio, washed again, then denatured and resolubilized by heating in 1.2% SDS–PBS to 95 °C for 5 min. Insoluble components were precipitated by centrifugation at 6,500g and soluble proteome was diluted in 5 ml 0.2% SDS–PBS. Labeled proteins were bound to streptavidin-agarose beads (170 μl resuspended beads per sample, ThermoFisher 20349) while rotating overnight at 4 °C. Bead-linked proteins were enriched by washing three times each in PBS and water, then resuspended in 6 M urea/PBS, reduced in TCEP (1 mM), alkylated with iodoacetamide (18 mM, ACROS AC122270050), before being washed and resuspended in 2 M urea/PBS and trypsinized overnight with 0.5 μg/pL sequencing grade trypsin (Promega

V5111). Tryptic peptides were eluted off. Beads were washed three times each in PBS and water, washed in TEV buffer solution (water, TEV buffer, 100 μM dithiothreitol (Invitrogen 15508013)) and resuspended in buffer with Ac-TEV protease (Invitrogen 12575-015) and incubated overnight. Peptides were diluted in water, acidified with formic acid (1.2 M, Fisher A117-50), and prepared for LC-MS/MS analysis.

IsoTOP-ABPP Mass Spectrometry Analysis—Peptides from all chemoproteomic experiments were pressure-loaded onto a 250 μm inner diameter fused silica capillary tubing packed with 4 cm of Aqua C18 reverse-phase resin (Phenomenex, 04A-4299), which was previously equilibrated on an Agilent 600 series high-performance liquid chromatograph using the gradient from 100% buffer A to 100% buffer B over 10 min, followed by a 5 min wash with 100% buffer B and a 5 min wash with 100% buffer A. The samples were then attached using a MicroTee PEEK 360 μm fitting (Thermo Fisher Scientific p-888) to a 13 cm laser pulled column packed with 10 cm Aqua C18 reverse-phase resin and 3 cm of strong-cation exchange resin for isoTOP-ABPP studies. Samples were analyzed using an Q Exactive Plus mass spectrometer (ThermoFisher Scientific) using a five-step Multidimensional Protein Identification Technology (MudPIT) program, using 0, 25, 50, 80 and 100% salt bumps of 500 mM aqueous ammonium acetate and using a gradient of 5–55% buffer B in buffer A (buffer A: 95:5 water:acetonitrile, 0.1% formic acid; buffer B 80:20 acetonitrile:water, 0.1% formic acid). Data were collected in data-dependent acquisition mode with dynamic exclusion enabled (60s). One full mass spectrometry (MS1) scan (400–1,800 mass-to-charge ratio (m/z)) was followed by 15 MS2 scans of the nth most abundant ions. Heated capillary temperature was set to 200 °C and the nanospray voltage was set to 2.75 kV.

Data were extracted in the form of MS1 and MS2 files using Raw Extractor v.1.9.9.2 (Scripps Research Institute) and searched against the Uniprot human database using ProLuCID search methodology in IP2 v.3-v.5 (Integrated Proteomics Applications, Inc.) [28]. Cysteine residues were searched with a static modification for carboxyaminomethylation (+57.02146) and up to two differential modifications for methionine oxidation and either the light or heavy TEV tags (+464.28596 or +470.29977, respectively). Peptides were required to be fully tryptic peptides and to contain the TEV modification. ProLUCID data were filtered through DTASelect to achieve a peptide false-positive rate below 5%. Only those probe-modified peptides that were evident across two out of three biological replicates were interpreted for their isotopic light to heavy ratios. For those probe-modified peptides that showed ratios greater than two, we only interpreted those targets that were present across all three biological replicates, were statistically significant and showed good quality MS1 peak shapes across all biological replicates. Light versus heavy isotopic probe-modified peptide ratios are calculated by taking the mean of the ratios of each replicate paired light versus heavy precursor abundance for all peptide-spectral matches associated with a peptide. The paired abundances were also used to calculate a paired sample t-test P value to estimate constancy in paired abundances and significance in change between treatment and control. P values were corrected using the Benjamini–Hochberg method.

TMT-Based Quantitative Proteomic Profiling—HAP1 WT cells were treated with either DMSO vehicle or EN450 (50 μM) for 24 h and lysate was prepared as described above. Briefly, 25-100 μg protein from each sample was reduced, alkylated and tryptically digested overnight. Individual samples were then labeled with isobaric tags using commercially available TMTsixplex (ThermoFisher 90061) kits, in accordance with the manufacturer's protocols. Tagged samples (20 μg per sample) were combined, dried with SpeedVac, resuspended with 300 μL 0.1% TFA in H2O, and fractionated using high pH reversed-phase peptide fractionation kits (ThermoFisher 84868) according to manufacturer's protocol. Fractions were dried with SpeedVac, resuspended with 50 μL 0.1% FA in H20, and analyzed by LC-MS/MS as described below.

Quantitative TMT-based proteomic analysis was performed as previously described using a Thermo Eclipse with FAIMS LC-MS/MS [26]. Acquired MS data was processed using ProLuCID search methodology in IP2 v.3-v.5 (Integrated Proteomics Applications, Inc.) [28]. Trypsin cleavage specificity (cleavage at K, R except if followed by P) allowed for up to 2 missed cleavages. Carbamidomethylation of cysteine was set as a fixed modification, methionine oxidation, and TMT-modification of N-termini and lysine residues were set as variable modifications. Reporter ion ratio calculations were performed using summed abundances with most confident centroid selected from 20 ppm window. Only peptide-to-spectrum matches that are unique assignments to a given identified protein within the total dataset are considered for protein quantitation. High confidence protein identifications were reported with a <1% false discovery rate (FDR) cut-off. Differential abundance significance was estimated using ANOVA with Benjamini-Hochberg correction to determine p-values.

Knockdown Studies—RNA interference was performed using siRNA purchased from Dharmacon. HAP1 cells were seeded at 100,000 cells per 6 cm plate and allowed to adhere overnight. Cells were transfected with 25 nM of either nontargeting (Dharmacon D-001810-10), anti-UBE2M (Dharmacon L-004348-00), or anti-UBE2D1 siRNA (Dharmacon L-0093870-00) using 7.5 μL of transfection reagent DharmaFECT 1 (Dharmacon T-2001-02) per well. For quadruple knockdown studies, 12.5 nM of anti-UBE2D1, -UBE2D2 (Dharmacon L-010383-00), -UBE2D3 (Dharmacon L-008478-00), and -UBE2D4 (Dharmacon L-009435-00) siRNA with 15 μL of DharmaFECT1 was used. Transfection reagent was added to OPTIMEM (ThermoFisher 31985070) media and allowed to incubate for 5 min at room temperature. Meanwhile siRNA was added to an equal amount of OPTIMEM. Solutions of transfection reagent and siRNA in OPTIMEM were then combined and allowed to incubate for 30 minutes at room temperature. These combined solutions were diluted with complete DMEM to provide 2 mL per well, and the media exchanged. Cells were incubated with transfection reagents for 48h, at which point the media was replaced with media containing DMSO or 50 μM EN450 and incubated for another 24 h. Cells were then harvested, and protein abundance analyzed by Western blotting.

Lentiviral overexpression of NFKB p105—In separate 15 mL conicals, 1 ug of expression clone cDNA (Origene RC208384L3) or control cDNA (Origene PS100093) was mixed with packaging plasmids MD2G (1 μg, Addgene 12259) and PSPAX2 (1 ug, Addgene

12260) in 600 μL per plate OPTIMEM and Lipofectamine™ 2000 transfection reagent (Invitrogen 11668027) was incubated with an equal volume of OPTIMEM (1:30 v/v) for 5 min prior to tubes being combined and incubated for 40 min at room temperature. The DNA-Lipofectamine™ mix was diluted with 8 mL of DMEM and added to HEK293T cells at 40% confluency in 10 cm plates. The next day, media was replaced with 6 mL fresh DMEM for 24 h.

For each control or expression clone, media was removed from HEK293T cells, filtered through a 0.45 micron syringe filter, mixed with 10 μL polybrene transfection reagent, and added to HAP1 WT cells at 50% confluency. HEK293T media was replaced with 6 mL fresh DMEM for 24 h and the infection process was repeated. 24 h after the second infection, the Hap1 WT infection media was removed and cells were seeded for proliferation experiments and Western blot analysis.

Transient overexpression of NFKB p105 in HEK293T cells—Prior to transfection, HEK293T cells were seeded into a 96-well plate (35,000 cells/well in 100 μL) or 6-well plate. Flag-tagged NFKB plasmid (Origene RC208384) or GFP control plasmid (Ward et. al, 2019) was diluted into Opti-MEM medium (0.2 ug DNA into 25 μL Opti-MEM per each well). Lipofectamine 2000 (Invitrogen, 11668019) was diluted into Opti-MEM I medium (0.5 μL Lipofectamine 2000 into 25 μL Opti-MEM I per each well). DNA and diluted Lipofectamine 2000 were combined in a 1:1 ratio then incubated at room temperature for 30 minutes. The DNA-Lipofectamine 2000 mixture was diluted with 50 μL of FBS-complete DMEM and then all 100 μL was added to each well. 24 hours post-transfection, media was carefully aspirated from each well, and 100 μL of fresh media containing either DMSO or compound was added, then assayed for proliferation. Briefly, for 6-well plate experiments, cells were seeded at 400,000 cells/well in 2 mL media, 4 μg of DNA and 10 μL of Lipofectamine 2000 per well were each diluted into 250 μL of Opti-MEM, and final transfection volume was 2 mL per well. Cells were analyzed via Western blot analysis after 48 hours.

***In vitro* pulldown of UBE2D1 with GST-tagged NFKB1—**Glutathione Sepharose 4B beads (1 μL of packed beads per sample, Cytiva 17075605) were washed 3 x with wash buffer (30 mM Tris (pH 7.5), 100 nM NaCl, 5 mM $MgCl_2$, 2 mM DTT, 0.1 mg/mL BSA, 10% glycerol, 0.01% Triton-X) with bead collection at 2000 x g between each wash, then resuspended in blocking buffer (30 mM 30 mM Tris (pH 7.5), 100 nM NaCl, 5 mM MgCl2, 2 mM DTT, 100 mg/mL BSA, 10% glycerol, 0.01% Triton-X) with gentle agitation at room temperature for 1 h, then washed twice more. GST-NFKB p105 (1 pmol per μL of beads, Novus H00004790-P01) in 100 μL was incubated with the beads for 2 h at 4° C with gentle agitation, then beads were washed three times. Beads were resuspended in wash buffer (45 μL per sample) containing 50 nM UBE2D1 (Boston Biochem Inc., E2-616-100) then aliquoted into PCR tubes. Input control was prepared via immediate addition of 15 μL Laemmli's buffer. Beads were treated with 5 μL of vehicle (10% DMSO, 0.25% CHAPS) or EN450 (50 μM) for a 50 μL final volume and incubated with gentle agitation at 4° C overnight. Beads were washed 4x with wash buffer (50 μL), resuspended in 20 μL of 1x

Laemmli's in PBS, boiled at 95° C for 5 min, pelleted at 1000 x *g* for 5 min, then analyzed via Western blotting.

***In vitro* ubiquitination assay—**UBE2D1 (5.2 μL, 25 μM, Boston Biochem. Inc., E2-616-100) was incubated with 0.5 μL of DMSO vehicle or EN450 (10 μM final concentration) for 30 min at 37 °C. Subsequently, UBE1 (0.95 μL, 1 μM, Boston Biochem. Inc., E-305-025) was added followed by Cul4A/RBX/NEDD8 (0.7 μL, 5 μM, Boston Biochem. Inc., E3-441-025), NFKB p105 (19.1 μL, 0.91 μM, Novus Biologicals, H00004790-Q01), FLAG-ubiquitin (0.5 μL, 10 mg/mL, Boston Biochem. Inc., U12001M), MgCl2 (0.5 μL, 500 mM), DTT (0.5 μL, 500 mM) and ATP (0.5 μL, 100 mM) to achieve a final volume of 25.5 μL. The mixture was incubated at 37 °C for 4 h with agitation. Then, 10 μL of Laemmli SDS sample loading buffer was added to quench the reaction and proteins were analyzed by Western Blot. All dilutions were made using 50 mM TBS (pH 7.5).

Synthetic Methods and Characterization for EN450 and EK-1-8

Preparation of *N*-(2-chloro-5-(*N*,*N*-dimethylsulfamoyl)phenyl)acrylamide:

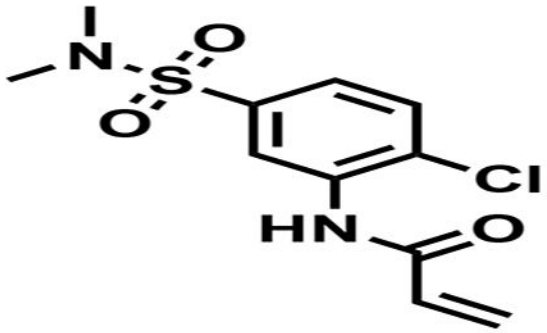

To a solution of dimethylamine (0.198 mL, 2.35 mmol) in DCM (5 mL) was added triethylamine (0.326 mL, 2.35 mmol) dropwise. The solution was stirred at 0 C for 45 min. Then, 3-nitro-4-chlorobenzenesulfonyl chloride (500 mg, 1.95 mmol) in 2:1 DCM/THF (5 mL) was added dropwise, and the solution was warmed to room temperature for 5 min when the reaction was diluted with DCM, washed with water, brine, dried over NaSO4, filtered, and the filtrate concentrated in vacuo. The residue was purified by flash chromatography on silica gel (0-30% EtOAc/Hexanes) to give the desired product 4-chloro-*N*,*N*-dimethyl-3-nitrobenzenesulfonamide (464 mg, 90%) as a light yellow solid. LCMS. ^{1}H NMR (400 MHz, $CDCl_3$) δ 8.27 (t, *J* = 2.2 Hz, 1H), 7.93 (dd, *J* = 8.4, 2.1 Hz, 1H), 7.78 (d, *J* = 8.4 Hz, 1H), 2.81 (d, *J* = 1.7 Hz, 6H). LCMS Rt 0.066 min; m/z 264.8 [M+H]

To a solution of ammonium chloride (346 mg, 6.46 mmol) in 1:1 EtOH/H2O (10 mL) was added iron powder (362 mg, 6.46 mmol). The solution was stirred at 60° C for 30 min. Then, 4-chloro-*N*,*N*-dimethyl-3-nitrobenzenesulfonamide (286 mg, 1.08 mmol) was added. The solution was stirred at 80 C for 1 hour, then diluted with DCM, washed with water, brine, dried over NaSO4, filtered, and the filtrate concentrated to give 3-amino-4-chloro-*N*,*N*-dimethylbenzenesulfonamide (183 mg, 78%) as a white powder. LCMS Rt 0.085 min; m/z 259.1 [M+H]

To a solution of 3-amino-4-chloro-*N,N*-dimethylbenzenesulfonamide (100 mg, 0.37 mmol) in DCM (15 mL) was added triethylamine (80 uL, 0.57 mmol) dropwise. The solution was stirred at 0 C for 5 min. Acryloyl chloride (67 uL, 0.83 mmol) was added and the solution was warmed to room temperature. After 2 hr, the mixture was diluted with water, extracted with DCM, washed with brine, dried over NaSO4, filtered, and the filtrate concentrated in vacuo. The residue was purified by flash chromatography on silica gel (20-50% EtOAc/Hexanes) to give *N*-(2-chloro-5-(*N,N*-dimethylsulfamoyl)phenyl)acrylamide (mg, %) as a white powder. ^{1}H NMR (500 MHz, $CDCl_3$) δ 8.91 (d, *J* = 2.1 Hz, 1H), 7.85 (s, 1H), 7.58 (d, *J* = 8.4 Hz, 1H), 7.52 (dd, *J* = 8.4, 2.2 Hz, 1H), 6.52 (dd, *J* = 16.8, 1.0 Hz, 1H), 6.35 (dd, *J* = 16.8, 10.2 Hz, 1H), 5.91 (dd, *J* = 10.2, 1.0 Hz, 1H), 2.80 (s, 6H).

^{13}C NMR (126 MHz, $CDCl_3$) δ 162.72, 134.80, 134.41, 129.77, 128.82, 128.75, 126.37, 123.05, 119.90, 37.33. HRMS calcd for C11H13ClN2O3S(M+H)+ 289.04137, found 289.04050

Preparation of *N*-(2-chloro-5-(*N,N*-dimethylsulfamoyl)phenyl)propionamide:

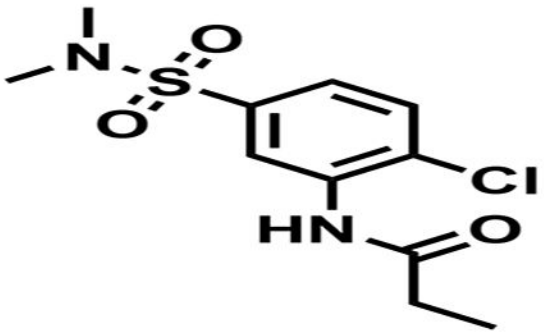

To a solution of 3-amino-4-chloro-*N,N*-dimethylbenzenesulfonamide (60 mg, 0.26 mmol) in DCM (5 mL) was added triethylamine (54 uL, 0.38 mmol) dropwise. The solution was stirred at 0 C for 5 min. Propionoyl chloride (25 uL, 0.28 mmol) was added and the solution was warmed to room temperature. After 10 min, the mixture was diluted with water, extracted with DCM, washed with brine, dried over NaSO4, filtered, and the filtrate concentrated in vacuo. The residue was purified by flash chromatography on silica gel (30-60% EtOAc/Hexanes) to give *N*-(2-chloro-5-(*N,N*-dimethylsulfamoyl)phenyl)acrylamide (48 mg, 65%) as a white powder.

^{1}H NMR (500 MHz, CDCl3) δ 8.79 (d, J = 2.3 Hz, 1H), 7.75 (s, 1H), 7.54 (d, J = 8.4 Hz, 1H), 7.47 (dd, J = 8.4, 2.2 Hz, 1H), 2.77 (s, 6H), 2.52 (q, J = 7.5 Hz, 2H), 1.29 (t, J = 7.5 Hz, 3H).

^{13}C NMR (126 MHz, CDCl3) δ 172.52, 135.58, 129.82, 127.37, 123.74, 120.99, 38.37, 31.19, 9.66. HRMS calcd for C11H15ClN2O3S(M+H)+ 291.05702, found 291.05624

Preparation of *N*-(2-chloro-5-(*N*-methyl-*N*-(prop-2-yn-1-yl)sulfamoyl)phenyl)acrylamide:

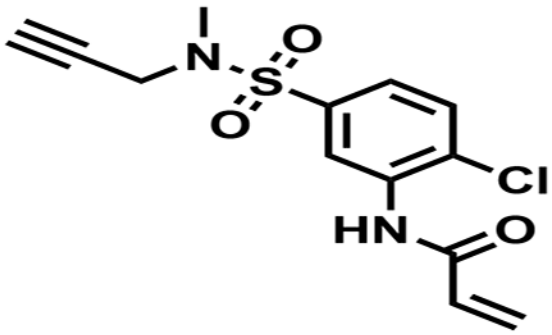

To a solution of *N*-methyl propargylamine (0.198 mL, 2.35 mmol) in DCM (5 mL) was added triethylamine (0.326 mL, 2.35 mmol) dropwise. The solution was stirred at 0 C for 45 min. Then, 3-nitro-4-chlorobenzenesulfonyl chloride (500 mg, 1.95 mmol) in 2:1 DCM/THF (5 mL) was added dropwise, and the solution was warmed to room temperature for 5 min when the reaction was diluted with DCM, washed with water, brine, dried over NaSO4, filtered, and the filtrate concentrated in vacuo. The residue was purified by flash chromatography on silica gel (0-30% EtOAc/Hexanes) to give the desired product 4-chloro-*N*-methyl-3-nitro-*N*-(prop-2-yn-1-yl)benzenesulfonamide (311 mg, 55%) as a light yellow solid. LCMS. m/z 288.1 [M+H]^{1}H NMR (500 MHz, $CDCl_3$) δ 8.36 (d, *J* = 2.2 Hz, 1H), 7.99 (dd, *J* = 8.4, 2.2 Hz, 1H), 7.75 (d, *J* = 8.5 Hz, 1H), 4.17 (d, *J* = 2.6 Hz, 2H), 2.92 (s, 3H), 2.26 – 2.11 (m, 1H). LCMS Rt 0.066 min; m/z 288.2 [M+H]

To a solution of ammonium chloride (350 mg, 6.46 mmol) in 1:1 EtOH/H2O (10 mL) was added iron powder (360 mg, 6.46 mmol). The solution was stirred at 60° C for 30 min. Then, 4-chloro-*N*-methyl-3-nitro-*N*-(prop-2-yn-1-yl)benzenesulfonamide (311 mg, 1.08 mmol) was added. The solution was stirred at 80 C for 1 hour, then diluted with DCM, washed with water, brine, dried over NaSO4, filtered, and the filtrate concentrated to give 3-amino-4-chloro-*N*-methyl-*N*-(prop-2-yn-1-yl)benzenesulfonamide (201 mg, 72%) as a white powder. H NMR (500 MHz, $CDCl_3$) δ 7.29 (s, 1H), 7.15 (d, *J* = 2.2 Hz, 1H), 7.01 (dd, *J* = 8.3, 2.2 Hz, 1H), 4.47 – 4.10 (m, 2H), 3.94 (d, *J* = 2.6 Hz, 2H), 2.76 (s, 3H), 2.11 – 2.06 (m, 1H). LCMS Rt 0.075 min; m/z 259.1 [M+H]

To a solution of 3-amino-4-chloro-*N*-methyl-*N*-(prop-2-yn-1-yl)benzenesulfonamide (100 mg, 0.37 mmol) in DCM (15 mL) was added triethylamine (70 uL, 0.50 mmol) dropwise. The solution was stirred at 0 C for 5 min. Acryloyl chloride (67 uL, 0.83 mmol) was added and the solution was warmed to room temperature. After 2 hr, the mixture was diluted with water, extracted with DCM, washed with brine, dried over NaSO4, filtered, and the filtrate concentrated in vacuo. The residue was purified by flash chromatography on silica gel (20-50% EtOAc/Hexanes) to give *N*-(2-chloro-5-(*N*-methyl-*N*-(prop-2-yn-1-yl)sulfamoyl)phenyl)acrylamide (116 mg, 97%) as a white powder. ^{1}H NMR (500 MHz, $CDCl_3$) δ 8.94 (s, 1H), 7.82 (s, 1H), 7.53 (d, *J* = 1.3 Hz, 2H), 6.49 (dd, *J* = 16.9, 1.1 Hz, 1H), 6.32 (dd, *J* = 16.9, 10.3 Hz, 1H), 5.88 (dd, *J* = 10.2, 1.1 Hz, 1H), 4.04 (d, *J* = 2.5 Hz, 2H), 2.90 (s, 3H), 2.10 (q, *J* = 3.1 Hz, 1H).

^{13}C NMR (126 MHz, $CDCl_3$) δ 163.24, 136.82, 134.96, 130.37, 129.35, 129.28, 127.09, 123.68, 120.58, 75.90, 74.11, 39.75, 34.44.

HRMS calcd for C13H13ClN2O3S(M+H)+ 313.04137, found 313.04053

Preparation of *N*-(2-chloro-5-(*N*-methyl-*N*-(prop-2-yn-1-yl)sulfamoyl)phenyl)propionamide:

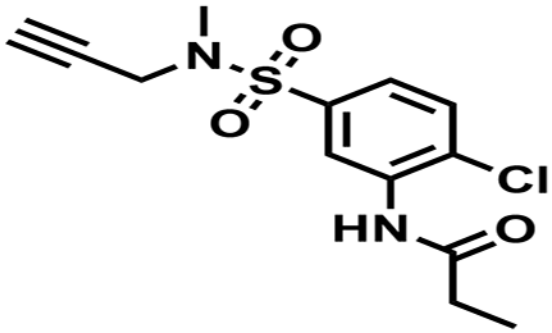

To a solution of 3-amino-4-chloro-*N*-methyl-*N*-(prop-2-yn-1-yl)benzenesulfonamide (50 mg, 0.19 mmol) in DCM (2 mL) was added triethylamine (78 uL, 0.56 mmol) dropwise. The solution was stirred at 0 C for 5 min. Propionyl chloride (50 uL, 0.56 mmol) was added and the solution was warmed to room temperature. After 10 min, the mixture was diluted with water, extracted with DCM, washed with brine, dried over NaSO4, filtered, and the filtrate concentrated in vacuo. The residue was purified by flash chromatography on silica gel (30-60% EtOAc/Hexanes) to give *N*-(2-chloro-5-(*N*-methyl-*N*-(prop-2-yn-1-yl)sulfamoyl)phenyl)propionamide (35 mg, 58%) as a white powder.

^{1}H NMR (500 MHz, CDCl3) δ 8.87 (s, 1H), 7.73 (s, 1H), 7.52 (d, J = 1.3 Hz, 2H), 4.05 (d, J = 2.5 Hz, 2H), 2.91 (s, 3H), 2.52 (q, J = 7.5 Hz, 2H), 2.12 (d, J = 2.5 Hz, 1H), 1.30 (t, J = 7.5 Hz, 3H).

^{13}C NMR (126 MHz, CDCl3) δ 171.87, 136.65, 135.08, 129.27, 126.85, 123.31, 120.48, 75.94, 74.06, 39.74, 34.41, 30.72, 9.15.

HRMS calcd for C13H15ClN2O3S(M+H)+ 315.05702, found 315.05641

Quantification and Statistical Analysis

Statistical details can be found in the figure legends as well as Supplemental Tables. Statistical analyses for TMT-based quantitative proteomics were performed as follows. High confidence protein identifications were reported with a <1% false discovery rate (FDR) cut-off. Differential abundance significance was estimated using ANOVA with Benjamini-Hochberg correction to determine p-values. IsoTOP-ABPP data analysis was performed as follows. Light versus heavy isotopic probe-modified peptide ratios are calculated by taking the mean of the ratios of each replicate paired light versus heavy precursor abundance for all peptide-spectral matches associated with a peptide. The paired abundances were also used to calculate a paired sample *t*-test *P* value to estimate constancy in paired abundances and significance in change between treatment and control. *P* values were corrected using the Benjamini–Hochberg method. All other statistical analyses were performed by Student's two-tailed t-tests.

Supplementary Material

Refer to Web version on PubMed Central for supplementary material.

Acknowledgement

We thank the members of the Nomura Research Group and Novartis Institutes for BioMedical Research for critical reading of the manuscript. This work was supported by Novartis Institutes for BioMedical Research and the Novartis-Berkeley Center for Proteomics and Chemistry Technologies (NB-CPACT) for all listed authors. This work was also supported by the Nomura Research Group and the Mark Foundation for Cancer Research ASPIRE Award for DKN, EAK. This work was also supported by grants by the National Science Foundation Molecular Foundations for Biotechnology Award (2127788) (for DKN) and the National Science Foundation Graduate Research Fellowship (for EAK). We also thank Drs. Hasan Celik, Alicia Lund, and UC Berkeley's NMR facility in the College of Chemistry (CoC-NMR) for spectroscopic assistance. Instruments in the CoC-NMR are supported in part by NIH S10OD024998.

Declaration of Interests

JAT, JMK, DD are employees of Novartis Institutes for BioMedical Research. This study was funded by the Novartis Institutes for BioMedical Research and the Novartis-Berkeley Translational Chemical Biology Institute. DKN is a co-founder, shareholder, and on the scientific advisory boards for Frontier Medicines and Vicinitas Therapeutics. DKN is a member of the board of directors for Vicinitas Therapeutics. DKN is also on the scientific advisory boards of The Mark Foundation for Cancer Research, Photys Therapeutics, Apertor Pharmaceuticals, Ecto Therapeutics, Oerth Bio, and Chordia Therapeutics. DKN is also on the investment advisory board of Droia Ventures.

References

1. Spradlin JN, Zhang E, and Nomura DK (2021). Reimagining Druggability Using Chemoproteomic Platforms. Acc. Chem. Res 54, 1801–1813. 10.1021/acs.accounts.1c00065. [PubMed: 33733731]
2. Dixon SJ, and Stockwell BR (2009). Identifying druggable disease-modifying gene products. Curr. Opin. Chem. Biol 13, 549–555. 10.1016/j.cbpa.2009.08.003. [PubMed: 19740696]
3. Bond MJ, and Crews CM (2021). Proteolysis targeting chimeras (PROTACs) come of age: entering the third decade of targeted protein degradation. RSC Chem. Biol 2, 725–742. 10.1039/d1cb00011j. [PubMed: 34212149]
4. Burslem GM, and Crews CM (2020). Proteolysis-Targeting Chimeras as Therapeutics and Tools for Biological Discovery. Cell 181, 102–114. 10.1016/j.cell.2019.11.031. [PubMed: 31955850]
5. Schreiber SL (2021). The Rise of Molecular Glues. Cell 184, 3–9. 10.1016/j.cell.2020.12.020. [PubMed: 33417864]
6. Mayor-Ruiz C, Bauer S, Brand M, Kozicka Z, Siklos M, Imrichova H, Kaltheuner IH, Hahn E, Seiler K, Koren A, et al. (2020). Rational discovery of molecular glue degraders via scalable chemical profiling. Nat. Chem. Biol 16, 1199–1207. 10.1038/s41589-020-0594-x. [PubMed: 32747809]
7. Backus KM, Correia BE, Lum KM, Forli S, Horning BD, González-Páez GE, Chatterjee S, Lanning BR, Teijaro JR, Olson AJ, et al. (2016). Proteome-wide covalent ligand discovery in native biological systems. Nature 534, 570–574. 10.1038/nature18002. [PubMed: 27309814]
8. Chung CY-S, Shin HR, Berdan CA, Ford B, Ward CC, Olzmann JA, Zoncu R, and Nomura DK (2019). Covalent targeting of the vacuolar H+−ATPase activates autophagy via mTORC1 inhibition. Nat. Chem. Biol 15, 776–785. 10.1038/s41589-019-0308-4. [PubMed: 31285595]
9. Meissner F, Geddes-McAlister J, Mann M, and Bantscheff M (2022). The emerging role of mass spectrometry-based proteomics in drug discovery. Nat. Rev. Drug Discov, 1–18. 10.1038/s41573-022-00409-3.
10. Spradlin JN, Hu X, Ward CC, Brittain SM, Jones MD, Ou L, To M, Proudfoot A, Ornelas E, Woldegiorgis M, et al. (2019). Harnessing the anti-cancer natural product nimbolide for targeted protein degradation. Nat. Chem. Biol 15, 747–755. 10.1038/s41589-019-0304-8. [PubMed: 31209351]

11. Vinogradova EV, Zhang X, Remillard D, Lazar DC, Suciu RM, Wang Y, Bianco G, Yamashita Y, Crowley VM, Schafroth MA, et al. (2020). An Activity-Guided Map of Electrophile-Cysteine Interactions in Primary Human T Cells. Cell 182, 1009–1026.e29. 10.1016/j.cell.2020.07.001. [PubMed: 32730809]
12. Baek K, Scott DC, and Schulman BA (2021). NEDD8 and ubiquitin ligation by cullin-RING E3 ligases. Curr. Opin. Struct. Biol 67, 101–109. 10.1016/j.sbi.2020.10.007. [PubMed: 33160249]
13. Weerapana E, Wang C, Simon GM, Richter F, Khare S, Dillon MBD, Bachovchin DA, Mowen K, Baker D, and Cravatt BF (2010). Quantitative reactivity profiling predicts functional cysteines in proteomes. Nature 468, 790–795. 10.1038/nature09472. [PubMed: 21085121]
14. Zhang X, Crowley VM, Wucherpfennig TG, Dix MM, and Cravatt BF (2018). Electrophilic PROTACs that degrade nuclear proteins by engaging DCAF16. bioRxiv, 443804. 10.1101/443804.
15. Henning NJ, Manford AG, Spradlin JN, Brittain SM, Zhang E, McKenna JM, Tallarico JA, Schirle M, Rape M, and Nomura DK (2022). Discovery of a Covalent FEM1B Recruiter for Targeted Protein Degradation Applications. J. Am. Chem. Soc 144, 701–708. 10.1021/jacs.1c03980. [PubMed: 34994556]
16. Zhang X, Luukkonen LM, Eissler CL, Crowley VM, Yamashita Y, Schafroth MA, Kikuchi S, Weinstein DS, Symons KT, Nordin BE, et al. (2021). DCAF11 Supports Targeted Protein Degradation by Electrophilic Proteolysis-Targeting Chimeras. J. Am. Chem. Soc 143, 5141–5149. 10.1021/jacs.1C00990. [PubMed: 33783207]
17. Belcher BP, Ward CC, and Nomura DK (2021). Ligandability of E3 Ligases for Targeted Protein Degradation Applications. Biochemistry. 10.1021/acs.biochem.1c00464.
18. Henning NJ, Boike L, Spradlin JN, Ward CC, Liu G, Zhang E, Belcher BP, Brittain SM, Hesse MJ, Dovala D, et al. (2022). Deubiquitinase-targeting chimeras for targeted protein stabilization. Nat. Chem. Biol 10.1038/s41589-022-00971-2.
19. Zhang X, Crowley VM, Wucherpfennig TG, Dix MM, and Cravatt BF (2019). Electrophilic PROTACs that degrade nuclear proteins by engaging DCAF16. Nat. Chem. Biol 15, 737–746. 10.1038/S41589-019-0279-5. [PubMed: 31209349]
20. Y C, and L S (2022). Inhibition of NEDD8 NEDDylation induced apoptosis in acute myeloid leukemia cells via p53 signaling pathway. Biosci. Rep 42. 10.1042/BSR20220994.
21. Chaturvedi MM, Sung B, Yadav VR, Kannappan R, and Aggarwal BB (2011). NF-κB addiction and its role in cancer: 'one size does not fit all.' Oncogene 30, 1615–1630. 10.1038/onc.2010.566. [PubMed: 21170083]
22. Baek K, Krist DT, Prabu JR, Hill S, Klügel M, Neumaier L-M, von Gronau S, Kleiger G, and Schulman BA (2020). NEDD8 nucleates a multivalent cullin–RING–UBE2D ubiquitin ligation assembly. Nature 578, 461–466. 10.1038/s41586-020-2000-y. [PubMed: 32051583]
23. Stabicki M, Kozicka Z, Petzold G, Li Y-D, Manojkumar M, Bunker RD, Donovan KA, Sievers QL, Koeppel J, Suchyta D, et al. (2020). The CDK inhibitor CR8 acts as a molecular glue degrader that depletes cyclin K. Nature 585, 293–297. 10.1038/s41586-020-2374-x. [PubMed: 32494016]
24. Forte N, Dovala D, Hesse MJ, McKenna JM, Tallarico JA, Schirle M, and Nomura DK (2022). Targeted Protein Degradation through E2 Recruitment. 2022.12.19.520812. 10.1101/2022.12.19.520812.
25. Lazear MR, Remsberg JR, Jaeger MG, Rothamel K, Her H, DeMeester KE, Njomen E, Hogg SJ, Rahman J, Whitby LR, et al. (2022). Proteomic discovery of chemical probes that perturb protein complexes in human cells. 2022.12.12.520090. 10.1101/2022.12.12.520090.
26. Chen S, Lovell S, Lee S, Fellner M, Mace PD, and Bogyo M (2021). Identification of highly selective covalent inhibitors by phage display. Nat. Biotechnol 39, 490–498. 10.1038/s41587-020-0733-7. [PubMed: 33199876]
27. Spradlin JN, Hu X, Ward CC, Brittain SM, Jones MD, Ou L, To M, Proudfoot A, Ornelas E, Woldegiorgis M, et al. (2019). Harnessing the anti-cancer natural product nimbolide for targeted protein degradation. Nat. Chem. Biol 15, 747–755. 10.1038/s41589-019-0304-8. [PubMed: 31209351]
28. Grossman EA, Ward CC, Spradlin JN, Bateman LA, Huffman TR, Miyamoto DK, Kleinman JI, and Nomura DK (2017). Covalent Ligand Discovery against Druggable Hotspots

Targeted by Anti-cancer Natural Products. Cell Chem. Biol 24, 1368–1376.e4. 10.1016/j.chembiol.2017.08.013. [PubMed: 28919038]

29. Xu T, Park SK, Venable JD, Wohlschlegel JA, Diedrich JK, Cociorva D, Lu B, Liao L, Hewel J, Han X, et al. (2015). ProLuCID: An improved SEQUEST-like algorithm with enhanced sensitivity and specificity. J. Proteomics 129, 16–24. 10.1016/j.jprot.2015.07.001. [PubMed: 26171723]
30. Ward CC, Kleinman JI, Brittain SM, Lee PS, Chung CYS, Kim K, Petri Y, Thomas JR, Tallarico JA, McKenna JM, et al. (2019). Covalent ligands screening uncovers a RNF4 E3 ligase recruiter for targeted protein degradation applications. ACS Chem. Biol 14, 2430–2440. [PubMed: 31059647]
31. Schneider CA, Rasband WS, and Eliceiri KW (2012). NIH Image to ImageJ: 25 years of image analysis. Nat. Methods 9, 671–675. [PubMed: 22930834]

Highlights

- We use chemoproteomic platforms to discover a covalent molecular glue degrader.
- We identify a cysteine-reactive covalent glue degrader EN450
- EN450 glues together E2 ubiquitin conjugating enzyme UBE2D with NFKB1

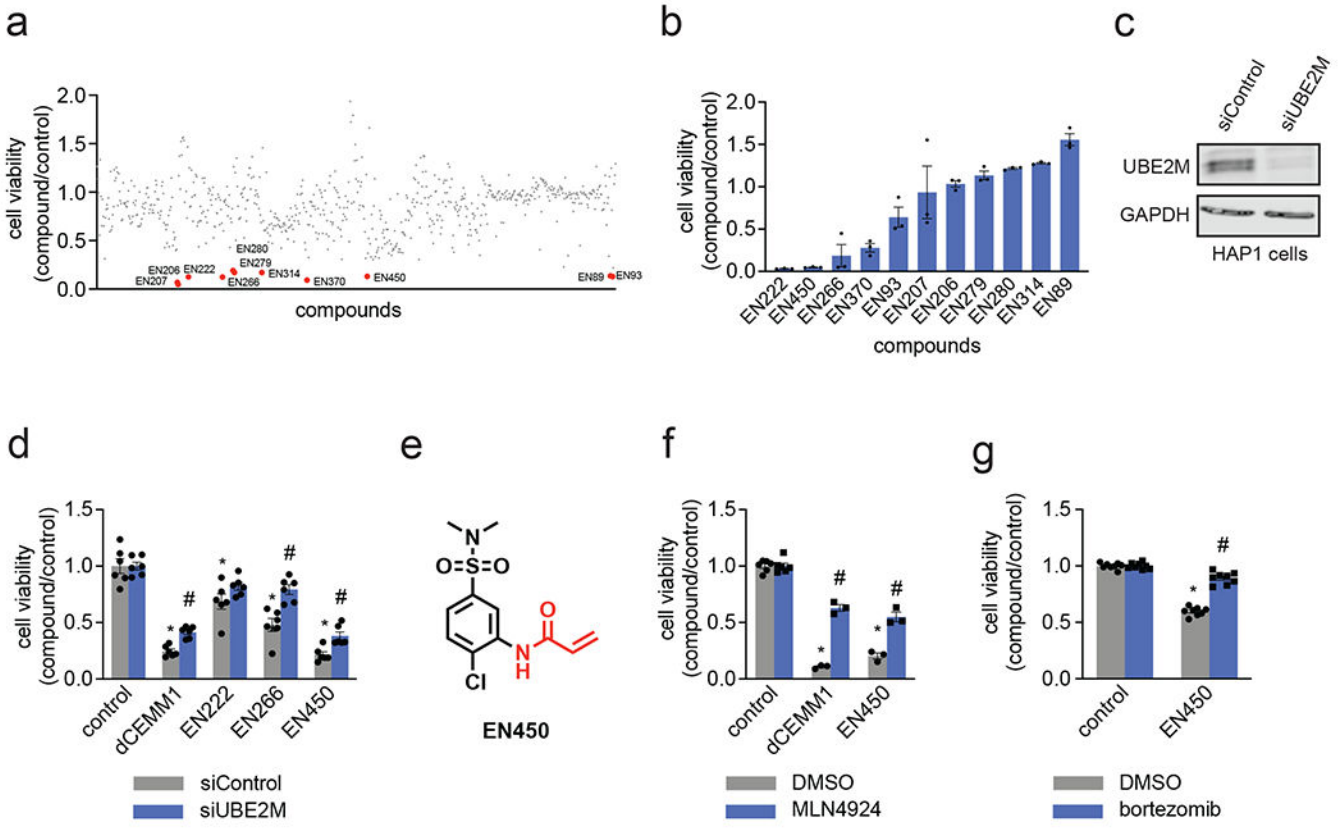

Figure 1. Discovery of a covalent molecular glue degrader with anti-proliferative activities in HAP1 leukemia cancer cells.

a) HAP1 cell viability screen of cysteine-reactive covalent ligands. DMSO vehicle or cysteine-reactive covalent ligands (50 μM) were treated in HAP1 cells for 24 h and cell viability was assessed by Hoescht staining. Compounds highlighted in red and labeled are those that impaired HAP1 cell viability by greater than 90 % compared to vehicle-treated controls. This screen was performed with n=1 biological replicate/group. (b) The 11 hit compounds from (a) were rescreened with n=3 biologically independent replicates/group in HAP1 cells under the same conditions. Individual replicate values shown. Among these hits EN222, EN226, and EN450 showed reproducible impaired HAP1 cell viability of greater than 90 % compared to DMSO vehicle-treated controls. (c) Knockdown of UBE2M. HAP1 cells were transiently transfected with siControl or siUBE2M oligonucleotides and knockdown of UBE2M was assessed by Western blotting compared to GAPDH loading control. (d) HAP1 cell viability in siControl and siUBE2M cells treated with DMSO vehicle, the positive control molecular glue degrader dCEMM1, EN222, EN266, or EN450 (50 μM) for 24 h, assessed by Hoescht staining. (e) structure of EN450 with the reactive acrylamide handle highlighted in red. (f) Attenuation of HAP1 cell viability impairments by NEDDylation inhibitor MLN4924. HAP1 cells were pre-treated with DMSO vehicle or MLN4924 (1 μM) for 1 h prior to treatment of cells with DMSO vehicle, dCEMM1, or EN450 (50 μM) for 24 h, and cell viability was assessed by Hoechst staining. (g) Attenuation of HAP1 cell viability impairments by proteasome inhibitor bortezomib. HAP1 cells were pre-treated with DMSO vehicle or bortezomib (1 μM) for 1 h prior to treatment

of cells with DMSO vehicle or EN450 (50 μM) for 24 h, and cell viability was assessed by Hoechst staining. Data in (d, f, g) are average ± sem of n=3-6 biologically independent replicates/group with individual replicate values also shown. Statistical significance is expressed as *$p<0.05$ compared to siControl or DMSO control groups in (d, f, g), #$p<0.05$ compared to corresponding siControl or DMSO pre-treated treatment groups, and calculated with Student's unpaired two-tailed t-tests. Related to Table S1.

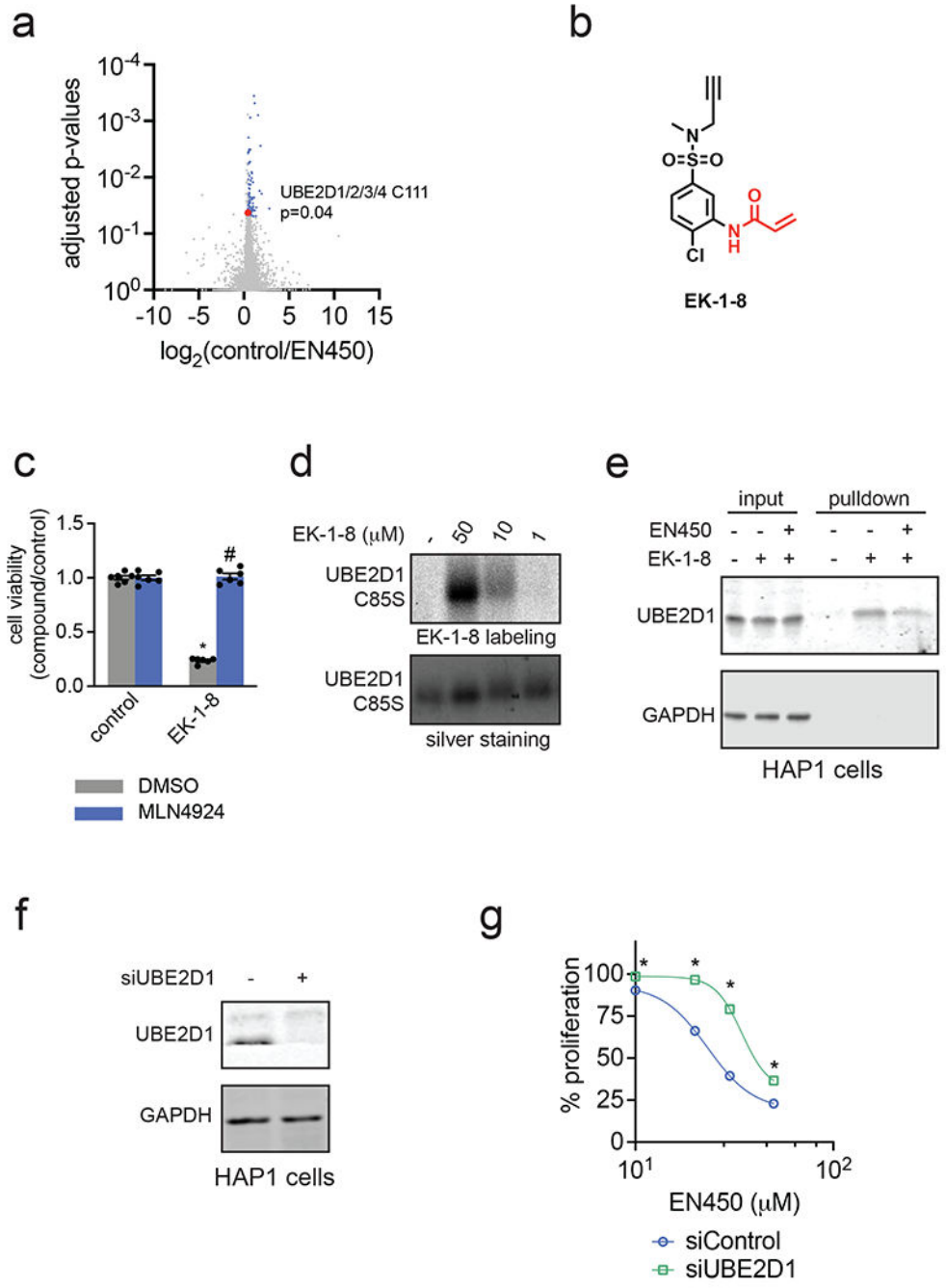

Figure 2. Chemoproteomic profiling and validation of EN450 targets in HAP1 cells.

(a) Cysteine chemoproteomic profiling of EN450 targets in HAP1 cells using isoTOP-ABPP. HAP1 cells were treated with DMSO vehicle or EN450 (50 μM) for 3 h, after which resulting cell lysates were labeled with an alkyne-functionalized iodoacetamide cysteine-reactive probe (200 μM) for 1 h, and an isotopically light (for DMSO) or heavy (for EN450) biotin-azide handle bearing a TEV protease recognition peptide was appended by CuAAC. Control and treated proteomes were combined in a 1:1 ratio, taken through the isoTOP-ABPP procedure and light/heavy probe-modified peptides were analyzed by LC-MS/MS

and quantified. Shown in blue are probe-modified peptides with light/heavy ratios >1.3 with adjusted $p<0.05$. Shown in red is C111 of UBE2D. Data shown are average ratios from n=4 biologically independent replicates/group. (b) structure of alkyne-functionalized probe derivative of EN450—EK-1-8 with cysteine-reactive acrylamide warhead highlighted in red. (c) Attenuation of HAP1 cell viability impairments by NEDDylation inhibitor MLN4924. HAP1 cells were pre-treated with DMSO vehicle or MLN4924 (1 μM) for 1 h prior to treatment of cells with DMSO vehicle, EK-1-8 (100 μM) for 24 h, and cell viability was assessed by Hoechst staining. (d) EK-1-8 labeling of recombinant pure human UBE2D1 C85S mutant protein. UBE2D1 C85S mutant protein was labeled with DMSO vehicle or EK-1-8 for 30 min, after which an azide functionalized rhodamine handle was appended onto probe-labeled protein by CuAAC, after which proteins were resolved by SDS/PAGE and visualized by in-gel fluorescence. Protein loading was assessed by silver staining. Gels are representative of an n=3 biologically independent replicates/group. (e) UBE2D1 pulldown from HAP1 cells with EK-1-8 probe. HAP1 cells were pre-treated with DMSO vehicle or EN450 (50 μM) for 1 h prior to treatment of cells with DMSO vehicle or EK-1-8 (10 μM) for 3 h. Probe-labeled proteins from resulting cell lysates were subsequently appended to an azide-functionalized biotin handle by CuAAC, avidin-enriched, eluted and separated by SDS/PAGE and blotted for UBE2D1 and unrelated protein GAPDH. Shown on the blot are also input UBE2D1 and GAPDH protein levels between the three groups shown. Blots are representative of an n=3 biologically independent replicates/group. (f) Confirmation of UBE2D1 knockdown. HAP1 cells were transiently transfected with siControl or siUBE2D1 oligonucleotides and UBE2D1 and loading control GAPDH expression were assessed after 72 h by Western blotting. Blot is representative of n=3 biologically independent replicates/group. (g) Percent HAP1 cell proliferation in siControl and siUBE2D1 cells treated with EN450 for 24 h compared to DMSO vehicle-treated controls. Data shown in (c) and (g) are average ± sem of n=6-30 biologically independent replicates/group with individual replicate values also shown. Statistical significance in (c) is expressed as $*p<0.05$ compared to DMSO-pre-treated control groups and $\#p<0.05$ compared to DMSO-pre-treated EK-1-8-treated groups and in (g) is expressed as $*p<0.05$ compared to the corresponding treatment group in siControl cells. Related to Table S2, Figure S1, and Figure S2.

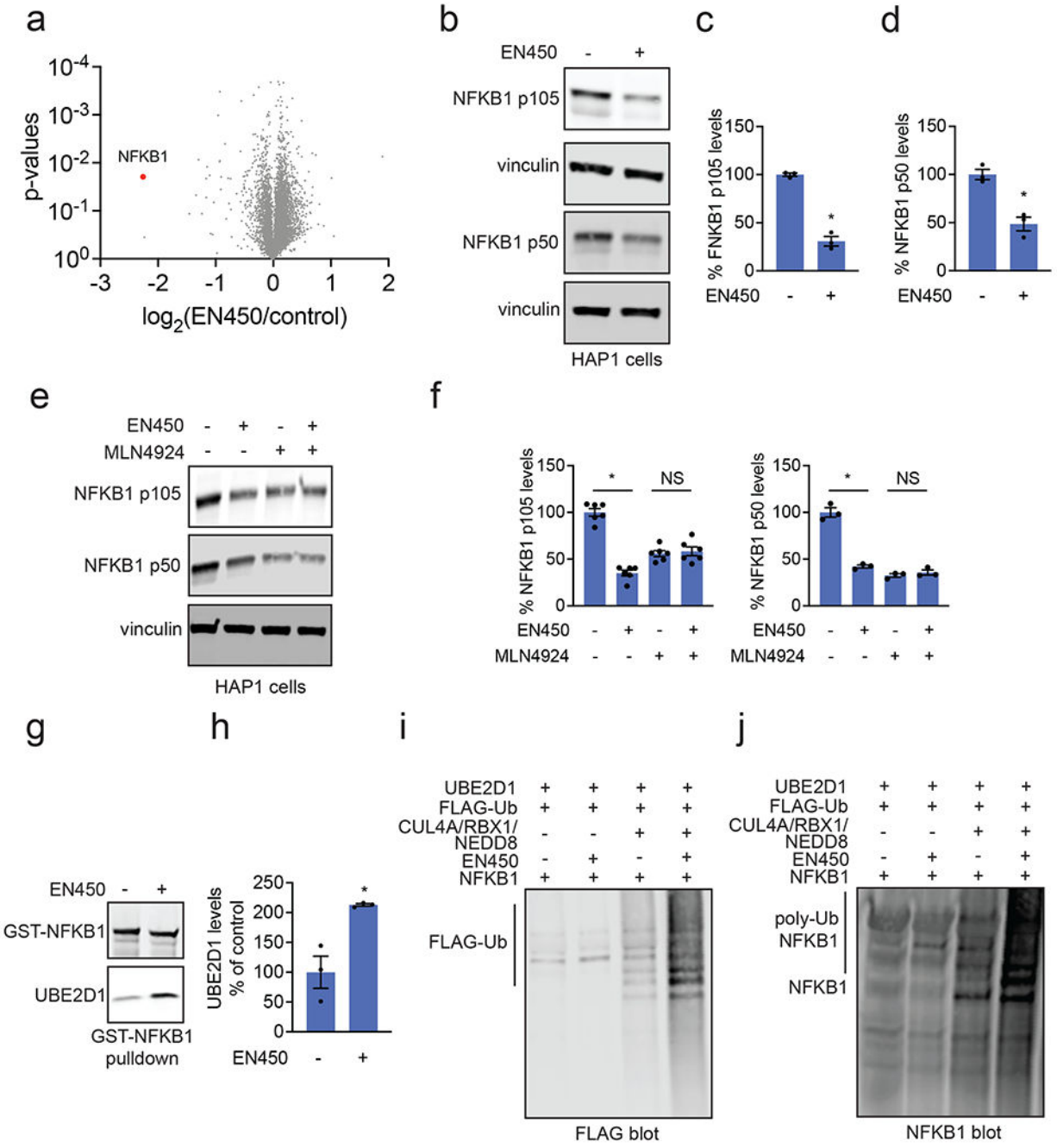

Figure 3. Identification of the protein degraded by EN450.

(a) TMT-based quantitative proteomic profiling of EN450 in HAP1 cells. HAP1 cells were treated with DMSO vehicle or EN450 (50 μM) for 24 h. Shown in red is the only protein reduced in levels by >4-fold with p-value <0.05—NFKB1. Data shown are from n=3 biologically independent replicates/group. (b) Western blotting analysis of p105 and p50 isoforms of NFKB1 and loading control vinculin levels in HAP1 cells treated with DMSO vehicle or EN450 (50 μM) for 24 h. (c, d) Quantification of experiment described in (b). (e) NEDDylation inhibitor attenuates NFKB1 loss by EN450 treatment in HAP1 cells. HAP1

cells were pre-treated with DMSO vehicle or MLN4924 (1 μM) for 1 h prior to treatment of cells with DMSO vehicle or EN450 (50 μM) for 24 h. NFKB1 and loading control vinculin levels were assessed by Western blotting. (f) Quantification of experiment described in (e). (g) Ternary complex formation between UBE2D1, EN450, and NFKB1. Recombinant pure human GST-NFKB1 and UBE2D1 proteins were incubated with DMSO vehicle or EN450 (50 μM) for 1 h, after which GST-NFKB1 was enriched and the pulldown eluate was blotted for NFKB1 and UBE2D1. (h) Quantification of pulldown experiment described in (g). (i, j) Ubiquitination assay with UBE2D1, ATP, FLAG-Ubiquitin, and NFKB1 pure proteins with the exclusion or addition of the CUL4A/RBX1/NEDD8 Cullin complex. This incubation was treated with DMSO vehicle or EN450 (50 μM) for 1 h. NFKB1 ubiquitination was detected by Western blotting visualizing FLAG-Ub in (i) and NFKB1 in (j). Blots shown in (b, e, g) are representative of n=3 biologically independent replicates/group. Data shown in (c, d, f, h) are average ± sem of n=3-8 biologically independent replicates/group with individual replicate values also shown. Statistical significance in (c, d, f, h) are expressed as *$p<0.05$ compared to DMSO vehicle-treated controls and NS denotes not significant. Related to Table S3 and Figure S3.

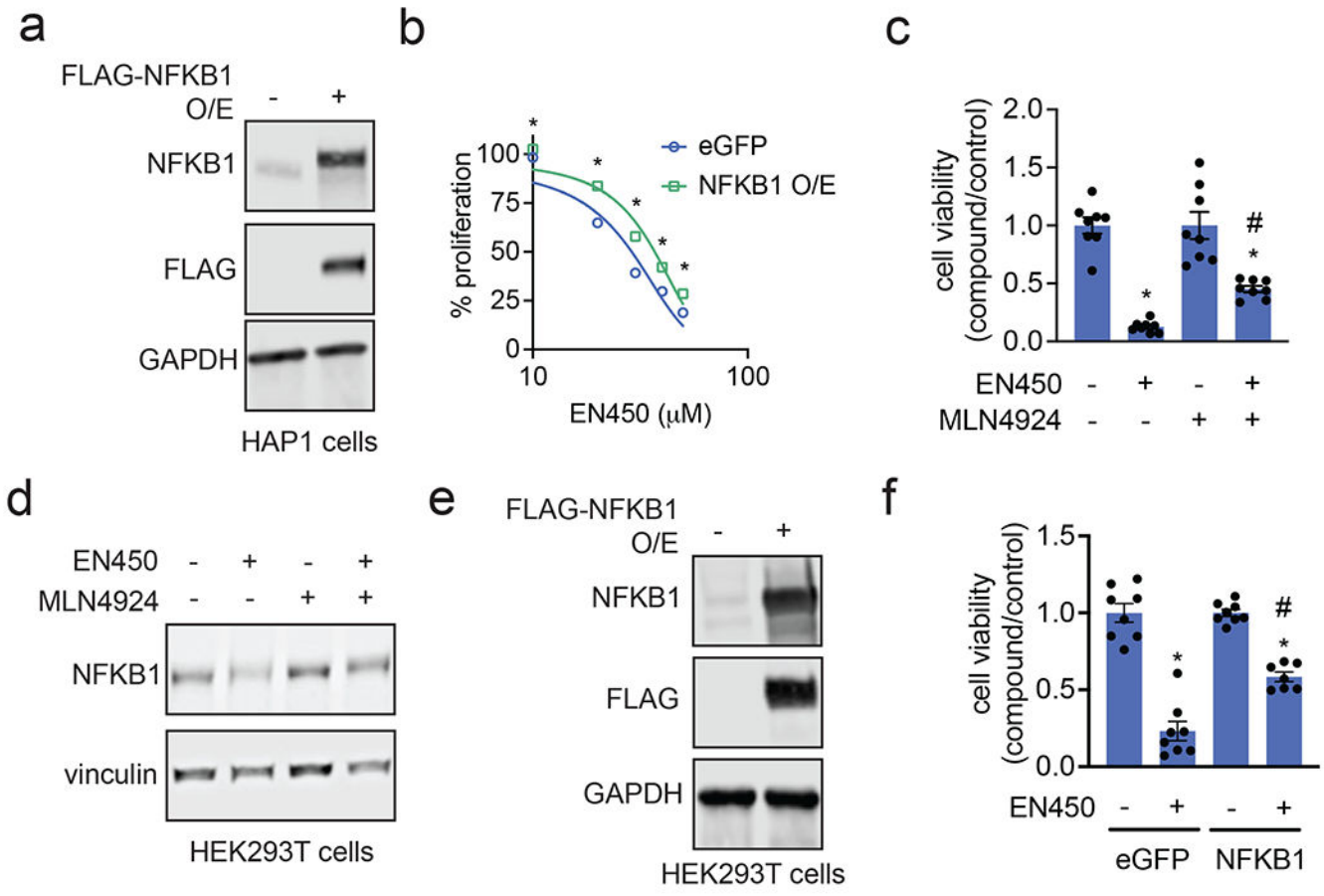

Figure 4. Understanding the role of NFKB1 in EN450-mediated effects.

(a) Stable lentiviral overexpression of FLAG-NFKB1 in HAP1 cells assessed by Western blotting for NFKB1, FLAG, and loading control GAPDH. (b) HAP1 eGFP control or FLAG-NFKB1 overexpressing cell viability from cells treated with DMSO vehicle or EN450 for 24 h. (c) Attenuation of HEK293T cell viability impairments by NEDDylation inhibitor MLN4924. HEK293T cells were pre-treated with DMSO vehicle or MLN4924 (1 μM) for 1 h prior to treatment of cells with DMSO vehicle or EN450 (50 μM) for 24 h, and cell viability was assessed by Hoechst staining. (d) NFKB1 and loading control vinculin levels in HEK293T cells pre-treated with DMSO vehicle or MLN4924 (1 μM) 1 h prior to treatment of cells with DMSO vehicle or EN450 (50 μM) for 24 h, assessed by Western blotting. (e) Transient transfection and overexpression of FLAG-NFKB1 in HEK293T cells assessed by Western blotting of NFKB1, FLAG, and loading control GAPDH. (f) HEK293T eGFP control or FLAG-NFKB1 overexpressing cell viability from cells treated with DMSO vehicle or EN450 (50 μM) for 24 h. Blots shown in (a, d, e) are representative of n=3 biologically independent replicates/group. Data shown in (c, f) are average ± sem of n=3-8 biologically independent replicates/group with individual replicate values also shown. Statistical significance in (c, f) are expressed as *p<0.05 compared to DMSO vehicle-treated controls or eGFP-expressing control cells and as #p<0.05 compared to DMSO pre-treated EN450-treated groups in (c) or EN450-treated eGFP-expressing cells in (f).

Key resources table

REAGENT or RESOURCE	SOURCE	IDENTIFIER
Antibodies		
Rabbit monoclonal anti-NFKB p105/p52	Abcam	Cat#ab323670; RRID:AB_776748
Rabbit monoclonal anti-SFT	Abcam	Cat#ab176561
Mouse monoclonal anti-UBE2D2	Origene	Cat#TA806600; RRID:AB_2628172
Rabbit monoclonal anti-UBE2D3	Abcam	Cat#ab176568
Mouse monoclonal anti-UBE2D4	Invitrogen	Cat#MA5-27358; RRID:AB_2725609
Rabbit monoclonal anti-UBE2M/UBC12	Abcam	Cat#ab109507; RRID:AB_10892148
Rabbit monoclonal anti-DYKDDDDK tag	Cell Signaling Technology	Cat#14793; RRID:AB_2572291
Mouse monoclonal anti-vinculin	Bio-Rad	Cat#MCA465S; RRID:AB_2214389
Mouse monoclonal anti-GAPDH	Proteintech	Cat#60004-1-Ig; RRID:AB_2107436
Goat anti-mouse IgG IRDye 680RD Secondary Antibody	LI-COR	Cat#926-68070; RRID:AB_10956588
Goat anti-rabbit IgG IRDye 800CW Secondary Antibody	LI-COR	Cat#926-32211; RRID:AB_621843
Bacterial and virus strains		
One-Shot™ Stbl3™ Chemically Competent *E. coli*	Invitrogen	C737303
HI-Control BL21 (DE3) Chemically Competent Cells	Lucigen	60435-1
Biological samples		
Chemicals, peptides, and recombinant proteins		
Recombinant Human UbcH5a/UBE2D1 Protein, CF	Boston Biochem Inc.	Cat#E2-616-100
Recombinant Human Ubiquitin Activating Enzyme (UBE1), CF	Boston Biochem Inc.	Cat#E-305
Recombinant Human CUL4A/NEDD8/RBX1A Complex Protein, CF	Boston Biochem Inc.	Cat#E3-441
Recombinant Human FLAG-Ubiquitin Protein, CF	Boston Biochem Inc.	Cat#U-120
Recombinant Human UBE2D1 (1-147)	This paper	N/A
Recombinant Human UBE2D1 C85S	This paper	N/A
Recombinant Human UBE2D1 C85S/C111S	This paper	N/A
Recombinant Human NFkB p105/p50 GST (N-term) Protein	Novus	Cat#H00004790-P01
Pierce protease inhibitor mini tablets, EDTA-free	ThermoFisher Scientific	Cat#A32955
Covalent Ligand Library, see Table S1	Enamine	N/A
Hoechst 33342 dye	Invitrogen	H3570
Bortezomib	Calbiochem	Cat#5043140001; CAS: 179324-69-7

REAGENT or RESOURCE	SOURCE	IDENTIFIER
NAE Inhibitor, MLN4924	Calbiochem	Cat#5054770001; CAS: 951950-33-7
TAMRA-PEG4-Azide	Click Chemistry Tools, Inc.	Cat#AZ109-5
Biotin picolyl azide	Sigma-Aldrich	Cat#900912
Tris(2-carboxyethyl)phosphine, hydrochloride	Strem	Cat#15-7400; CAS:51805-45-9
Tris[(1-benzyl-1H-1,2,3-triazol-4-yl)methyl]amine	Sigma-Aldrich	Cat#678937; CAS:510758-28-8
Copper(II)sulfate	Sigma-Aldrich	Cat#451657; CAS:7758-98-7
High-capacity streptavidin agarose resin	ThermoFisher Scientific	Cat#20357
Laemmli SDS sample buffer, reducing (4x)	Alfa Aesar	Cat#J60015
Spectra multicolor broad range protein ladder	Thermo Scientific	Cat#26634
ReBlot Plus Strong Antibody Stripping Solution, 10x	Millipore	Cat#2504
N-Hex-5-ynyl-2-iodo-acetamide (IA-alkyne)	Chess Gmbh	Cat#3187; CAS:930800-38-7
Biotin-TEV-Azide	Weerapana et. al, 2010	N/A
Streptavidin agarose resin	ThermoFisher Scientific	Cat#20349
Iodoacetamide 98%	ACROS Organics	Cat#AC122270050; CAS:144-48-9
Sequencing grade modified trypsin, porcine	Promega	Cat#V511A
UltraPure Dithiothreitol	Invitrogen	Cat#15508013
AcTEV Protease	Invitrogen	Cat#12575-015
Formic acid, 99.0+%, optima LC/MS grade	Fisher Scientific	Cat#A117-50; CAS:64-18-6
TMTsixplex isobaric label reagent set	ThermoFisher Scientific	Cat#90061
Pierce high pH reversed-phase peptide fractionation kit	ThermoFisher Scientific	Cat#84868
Opti-MEM Reduced Serum Media	ThermoFisher Scientific	Cat#31985062
Lipofectamine 2000 Transfection Reagent	ThermoFisher Scientific	Cat#11668027
DharmaFECT 1	Dharmacon	Cat#T-2001-02
Glutathione Sepharose 4B beads	Cytiva	Cat#17075605
N-[2-chloro-5-(dimethylsulfamoyl)phenyl]prop-2-enamide	Enamine	Cat#EN300-7515212
Critical commercial assays		
Q5 Site Directed Mutagenesis Kit	New England BioLabs	Cat#E0554S
Deposited data		
isoTOP-ABPP and TMT quantitative proteomics data	PRIDE database	PXD039924
Experimental models: Cell lines		
Human: Hap1 parental cell line	Horizon	Cat#C859
Human: Hek293T	ATCC	CRL-3216
Experimental models: Organisms/strains		

REAGENT or RESOURCE	SOURCE	IDENTIFIER
Oligonucleotides		
siRNA: ON-TARGETplus Human UBE2D1 SMARTPool	Dharmacon	Cat#L-0093870-00
siRNA: ON-TARGETplus Human UBE2D2 SMARTPool	Dharmacon	Cat#L-010383-00
siRNA: ON-TARGETplus Human UBE2D3 SMARTPool	Dharmacon	Cat#L-008478-00
siRNA: ON-TARGETplus Human UBE2D4 SMARTPool	Dharmacon	Cat#L-009435-00
siRNA: ON-TARGETplus Non-targeting Pool	Dharmacon	Cat#D-001810-10
siRNA: ON-TARGETplus Human UBE2M SMARTPool	Dharmacon	Cat#L-004348-00
Recombinant DNA		
pMD2.G	Trono Lab Constitutive Lentiviral Plasmids (unpublished)	Addgene plasmid #12259; RRID: Addgene_12259
psPAX2	Trono Lab Constitutive Lentiviral Plasmids (unpublished)	Addgene plasmid #12260; RRID: Addgene_12260
pLenti-C-Myc-DDK-P2A-Puro NFKB1	Origene	Cat#RC208384L3
pLenti-C-mGFP-P2A-Puro	Origene	Cat#PS100093
pCMV6-Entry eGFP	Ward et. al, 2019	N/A
pCMV6-Entry NFKB1	Origene	Cat#RC208384
Software and algorithms		
ImageJ	Schneider et al., 2012	https://imagej.nih.gov/ij/
IP2 proteomics pipeline 5.0.1	Integrated Proteomics Applications	N/A
Other		